DISCLAIMER

PNL-SA--20305

DE92 015091

A COMPARATIVE EIS STUDY ON CERMET AND PLATINUM ANODES FOR THE ELECTROLYTIC PRODUCTION OF ALUMINUM

C. F. Windisch, Jr.

May 1992

Presented at the
Electrochemical Society 181st Meeting
May 17-22, 1992
St. Louis, Missouri

Work supported by
the U.S. Department of Energy
under Contract DE-AC06-76RLO 1830

Pacific Northwest Laboratory
Richland, Washington 99352

A COMPARATIVE EIS STUDY ON CERMET AND PLATINUM ANODES FOR THE ELECTROLYTIC PRODUCTION OF ALUMINUM

Charles F. Windisch Jr.

Pacific Northwest Laboratory[a]
Richland, WA 99352

ABSTRACT

Electrochemical impedance spectra (EIS) of NiO-$NiFe_2O_4$-Cu cermet anodes in alumina-saturated molten cryolite at anodic potentials above the decomposition potential of alumina exhibited a loop with a characteristic frequency of about 1 Hz. A similar feature was observed using platinum anodes under the same experimental conditions. Analysis of these data suggests the loop was due to gas bubbling. Features associated with charge-transfer processes were not sufficiently resolved to determine the corrosion properties of the cermet anode.

INTRODUCTION

Cermet anodes are currently being evaluated as candidate nonconsumable substitutes for carbon in Hall-Heroult cells for the commercial production of aluminum metal. To be acceptable, these cermet anodes must corrode or wear at a low rate under electrolysis conditions. A recent pilot-scale test of the cermet anode material showed that it is susceptible to corrosion under certain conditions. In this work, electrochemical impedance spectroscopy (EIS) was used to compare the electrochemical reactions occurring on a cermet anode with those occurring on platinum metal during electrolysis in alumina-saturated molten cryolite. The electrolytic production of oxygen gas is known to be the principal reaction for a platinum anode under these conditions. Thus, it was hoped that significant differences in EIS data for platinum and for the cermet anodes would suggest undesirable corrosion reactions for the cermet anode, and that lack of significant differences between data for the two materials would indicate that the cermet was largely "inert." Unfortunately, from the aspect of corrosion analysis, the electrochemical impedance spectra for both the cermet anode and the platinum anode were dominated by a loop that appears to be due to gas bubbling. The loop obscured the characteristics of the charge-transfer process. Nevertheless, the EIS spectra are significant in that they are some of the first obtained on the behavior of gas-generating electrodes in a molten salt.

---

[a]The Pacific Northwest Laboratory is operated by Battelle Memorial Institute for the U.S. Department of Energy under Contract DE-AC06-76RLO 1830.

EXPERIMENTAL

Cermet anodes of the type NiO-$NiFe_2O_4$-Cu were prepared from a spray-dried oxide powder blend fabricated by Stackpole, Inc., Pittsburgh, Pennsylvania (synthesized from 51.7 wt% NiO and 48.3 wt% Fe_2O_3) and Cu metal at 17 wt% of the cermet product, using methods reported previously (1). The cylindrical anodes were sheathed with boron nitride to expose only the bottom 1 cm^2 of surface area to the electrolyte. Platinum anodes were made from 1/8-in-diameter rod obtained from Johnson Matthey, Inc. (Seabrook, New Hampshire). The electrolyte was composed of natural Greenland cryolite and excess AlF_3 to give a bath ratio (NaF/AlF_3 in wt%) equal to 1.15, 5.5 wt% CaF_2, 1.0 wt% MgF_2, and Al_2O_3 at 8.0 wt% (saturation). The electrolyte composition is representative of the bath compositions used in commercial aluminum production facilities. The bath temperature was 983°C.

Electrochemical impedance spectra were obtained using a Solartron 1286 Electrochemical Interface and Solartron 1250 Frequency Response Analyzer. A three-electrode system was used with the anode as the working electrode, the graphite crucible as the counter electrode, and an Al/Al_2O_3 reference electrode. The reference electrode was based on a reported design (2) but was in an electrolyte with the same composition as the anode. Impedance measurements were made at various anodic potentials with respect to the Al/Al_2O_3 reference over the frequency range 0.1 Hz to 10 kHz using a ±10 mV excitation signal.

RESULTS AND DISCUSSION

The complex impedance spectra for the cermet anode at current densities of 0.44 A cm^{-2} and 0.80 A cm^{-2} are shown in Figs. 1a and 1b, respectively. Plots for the platinum anode at current densities of 0.53 A cm^{-2} and 1.0 A cm^{-2} are shown in Figs. 2a and 2b, respectively.

The spectra are very similar. Each plot exhibits a loop at low frequencies with a characteristic frequency of about 1 Hz. The diameters of these loops appear to increase with increasing current density from about 0.07 ohm cm^2 at 0.44 A cm^{-2} to 0.10 ohm cm^2 at 0.80 A cm^{-2} in the case of the cermet anode, and from approximately 0.10 ohm cm^2 at 0.53 A cm^{-2} to 0.15 ohm cm^2 at 1.0 A cm^{-2} in the case of the platinum anode.

The spectra also show features at higher frequencies (>10 Hz). The high-frequency features are very small and were difficult to resolve; however, they are clearer at the lower current density than at the higher current density for both the cermet anode and the platinum anode. At the lower current densities, they appeared to be semicircular. At the higher current densities, the high-frequency features appear smaller and are obscured (completely, in the case of platinum) by the low-frequency loops.

The high-frequency and low-frequency Z'-intercepts, given by Z'_{hf} and Z'_{lf} respectively, were estimated by extrapolation from Figs. 1 and 2 and are listed in Table I. Z'_{hf} and Z'_{lf} increased with increasing current density for both anodes.

Table I. Impedances and Overvoltages for Anodes

Anode	Current (I)	Z'_{hf}	Z'_{lf}	IR_e	Slope	η
	(A cm^{-2})	(ohm cm^2)	(ohm cm^2)	(V)	(V)	(V)
Cermet	0.44	0.30	0.42	0.13	0.42	0.07
	0.80	0.36	0.50	0.29	0.53	0. 11
Platinum	0.53	0.25	0.37	0.13	0.35	0. 07
	1.0	0.31	0.46	0.31	0.49	0. 09

Z'_{lf} is the sum of at least three components according to Figs. 1 and 2. These components are Z'_{hf}, the "resistance" of the high-frequency process(es) that give(s) rise to the poorly defined high frequency loop(s), and the "resistance" of the low-frequency process giving rise to the low-frequency loop. The latter is equal in magnitude to the diameter of the low-frequency loop.

Z'_{hf} can be equated with the electrolyte resistance, R_e. The voltage drop through the electrolyte was computed for each anode as the product of the current density, I, and R_e. As shown in Table I, the the voltage drop through the electrolyte also increased with current density for both the cermet anode and the platinum anode.

Plots of IR_e versus I for the platinum and cermet anodes are shown in Fig. 3. Additional Z' data collected in this laboratory at 10 kHz and at other current densities are also included. The curves are non-linear almost certainly due to the increase in gas volume (from bubbles) at higher current densities. The variation of the voltage drop due to changes in bubble configuration with current density at a given current density is therefore given by the local slope of the IR_e versus I curve. This slope, which is listed in Table I for the platinum and cermet anodes at the various current densities, contains the additional resistance associated with the change in bubble configuration accompanying a small change in current density. As shown in Table I, the value for the slope is very close to the magnitude of Z'_{lf} for each of the conditions studied. At a sufficiently low excitation frequency (<1 Hz), the EIS data "capture" the effect of the bubble configuration on the overall impedance. The EIS-derived impedances also include contributions from the electrochemical transformations, but their effects are very small, especially at the higher current densities, as indicated by the size of the high-frequency features in Figs. 1a and 2a.

Given the important role the bubble configuration plays in determining Z_{lf} and, consequently, the dc overpotential, the most likely source of the low-frequency loop is the bubbling processes itself. At frequencies significantly above 1 Hz, the bubble configuration is frozen; at frequencies significantly below 1 Hz, the impedance contains an additional "bubble resistance." At intermediate frequencies, the bubble configuration lags behind the current and a loop is obtained.

Other assignments for the low-frequency loop seem implausible. The loop has a "capacitance" on the order of 10^4 μF cm^{-2}, which suggests it is not associated with a simple charge-transfer process. The apparent increase in diameter of the low-frequency

loop with current density is also inconsistent with a simple Faradaic process that predicts a resistance inversely proportional to current. The fact that the relaxation time is about 1 s also argues against an adsorption process. Given the limited number of platinum atoms available on the surface, the adsorption would have to occur at a much faster rate to support the experimental current densities which are on the order of 1 A cm^{-2}.

The very small features in the complex impedance spectra at higher frequencies may be due to the charge-transfer processes, but this is uncertain since the features were poorly resolved and obscured by the low-frequency loop. Unfortunately, this result limits the utility of the electrochemical impedance data in comparing the electrochemical reactions at the cermet and platinum anodes. With the present sensitivity of the technique, it appears that the data simply indicate that both anodes are producing bubbles.

Overvoltages, η, calculated from the impedance data and given in Table I,[b] are also inconclusive. The values for the overvoltages on platinum differ significantly from those reported by Thonstad (4) and, taken together with the observed differences in the IR_e versus I curves for the platinum and cermet anodes (Fig. 3), seem to indicate a dependence on cell geometry, anode shape and, possibly, anode surface structure (e.g. roughness). This is not surprising because the magnitude of the "bubble effect" is also expected to vary with these parameters. Studies on carbon anodes have shown similar effects (5). Given the need to keep power losses as low as possible in large-scale aluminum reduction cells, particularly in the case of inert anodes where the thermodynamic decomposition potential is high (relative to carbon anodes), further work would seem warranted to sort out the roles of these important variables on overvoltage.

CONCLUSIONS

Electrochemical impedance spectra for both NiO-$NiFe_2O_4$-Cu cermet anodes and platinum anodes exhibited a loop with a characteristic frequency of about 1 Hz when polarized in alumina-saturated molten cryolite at potentials above the decomposition potential of alumina. Analysis of these data suggests the loop was due to gas bubbling. Features associated with charge-transfer processes were not sufficiently resolved to determine the corrosion properties of the cermet material.

ACKNOWLEDGMENTS

This work was supported by the Office of Industrial Processes, U. S. Department of Energy, Washington, DC. The author acknowledges the managerial guidance by M. J. McMonigle at the USDOE, and the laboratory assistance by N. D. Stice at PNL. The author is also grateful for suggestions and comments provided by Dr. E. W. Dewing and Dr. W. E. Haupin.

---

[b]The overvoltages were calculated by subtracting the voltage drop through the electrolyte, IR_e, and the decomposition potential for alumina, 2.20 V versus Al/Al_2O_3 (3), from the observed anode potential relative to Al/Al_2O_3.

REFERENCES

1. P. E. Hart, "Inert Anode/Cathode Program Fiscal Year 1986 Annual Report," PNL-6247, Pacific Northwest Laboratory, Richland, WA (1987).

2. J. W. Brugman, J. A. Leistra, and P. J. Sides, *J. Electrochem. Soc.*, **133**, 496 (1986).

3. K. Grjotheim, C. Krohn, M. Malinovsky, K. Matisasovsky, and J. Thonstad, "Aluminium Electrolysis," p. 196, Aluminium-Verlag, Dusseldorf (1982).

4. J. Thonstad, *Electrochim. Acta*, **13**, 449 (1968).

5. E. W. Dewing and E. Th. van der Kouwe, *J. Electrochem. Soc.*, **122**, 358 (1975).

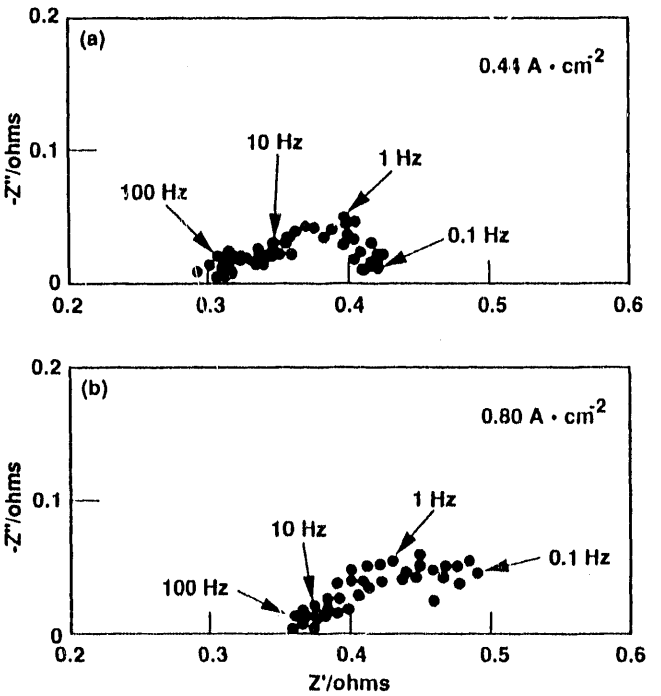

Fig. 1. Electrochemical impedance spectra for cermet anode at (a) 0.44 A cm^{-2} and (b) 0.80 A cm^{-2} in alumina-saturated molten cryolite at 983°C.

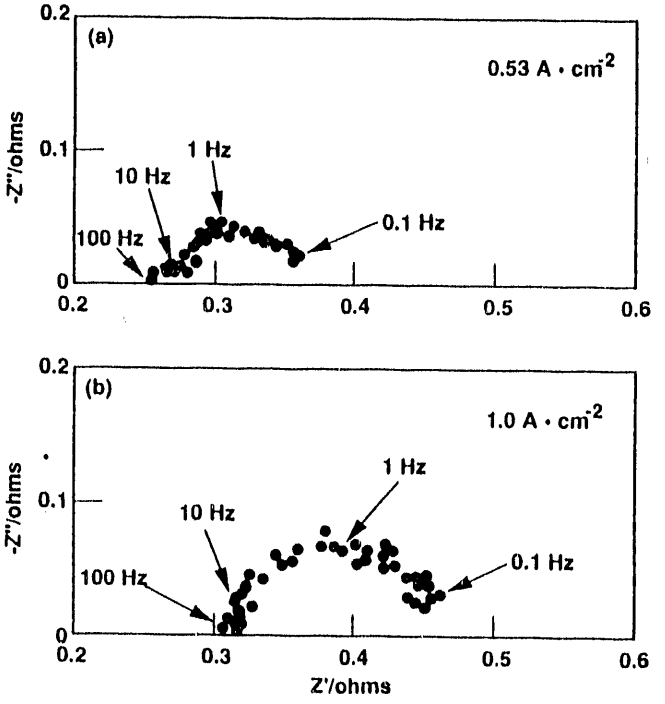

Fig. 2. Electrochemical impedance spectra for platinum anode at (a) 0.5 A cm-2 and (b) 1.0 A cm-2 in alumina-saturated molten cryolite at 983°C.

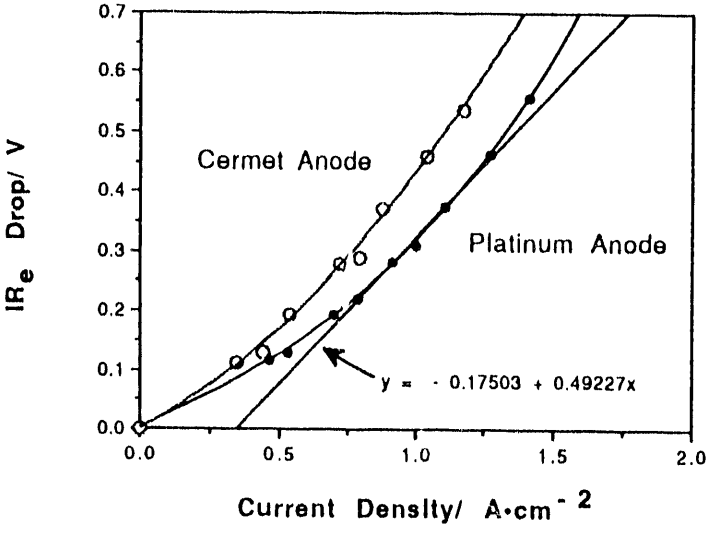

Fig. 3. Variation of the voltage through the electrolyte with current density for the cermet and platinum anodes. Local slope is shown for the platinum anode at 1 A cm-2.

END

DATE FILMED

7/23/92